Corrosion Versus Mechanical Tests for Indirect Detection of Alpha Prime Phase in UNS S32520 Super Duplex Stainless Steel

T.F. Fontes,[‡,] R. Magnabosco,[**] M. Terada,[***] A.F. Padilha,[***] and I. Costa[*]*

ABSTRACT

Alpha prime formation leads to material embrittlement and deterioration of corrosion resistance. In the present study, the mechanical and corrosion behavior of super duplex stainless steel UNS S32520 aged at 475°C from 0.5 h to 1,032 h was evaluated using microhardness measurements, Charpy impact tests, electrochemical impedance spectroscopy, and cyclic polarization curves. The sensibility of these tests to the effects of alpha prime phase was investigated. The microhardness test showed a gradual increase in hardness with aging time, whereas the impact tests revealed losses of about 80% in the energy absorption capacity for the material aged for 12 h in comparison with the solution-annealed samples. The most responsive analysis was the impact test, which indirectly revealed the presence of this deleterious phase in samples aged for 0.5 h. The electrochemical impedance spectroscopy and polarization tests were not highly sensitive to the alpha prime phase unless these are present in large amounts in the stainless steel.

KEY WORDS: Charpy impact tests, corrosion resistance, embrittlement, microhardness measurements, super duplex stainless steel

INTRODUCTION

Duplex stainless steels (DSS) have been used extensively in nuclear, chemical, and petroleum industries because of their good weldability, mechanical, and corrosion resistance, especially in aggressive environments.[1-6] These steels are basically Fe-Cr-Ni-Mo-N alloys presenting a microstructure of approximately 50 vol% ferrite and 50 vol% austenite. When the pitting resistance number (PREN = %Cr + 3.3 × %Mo + 16 × %N) assumes values greater than 40, the material is called super duplex stainless steel (SDSS).

Despite their superior mechanical and corrosion resistance properties, they are susceptible to precipitation of deleterious phases when exposed to specific temperatures, such as the chromium-enriched body-centered cubic (bcc) phase, called alpha prime. This phase leads to deterioration of mechanical and corrosion resistance properties. This precipitation process occurs in the temperature range from 270°C to 550°C, but it is most favored at 475°C and leads to material embrittlement.[7-17,4-5] This phase is formed in the ferrite matrix either by nucleation and growth processes or by spinodal decomposition.[7-8,18-21] Depending on their amount in the stainless steel, the corrosion resistance and absorbed energy in impact tests decrease whereas the hardness and mechanical strength increase.

Stainless steels usually present a ductile fracture behavior, characterized by dimple structures. However, when alpha prime precipitates, the ductile fracture turns into brittle structures, with a lot of cleavage surfaces from the blockage of dislocations movements and reduction of active slip planes.[22]

Submitted for publication July 6, 2010; in revised form, November 12, 2010.

‡ Corresponding author. E-mail: talita.filier@hotmail.com.
* Instituto de Pesquisas Energéticas e Nucleares, CCTM, Av. Lineu Prestes, 2242, CEP 05508-900, Cidade Universitária, Butantã, São Paulo-SP, Brazil.
** Ignatian Educational Foundation – FEI, Mechanical Engineering Department, Av. Humberto Alencar Castelo Branco, 3972, CEP 09850-901, Bairro Assunção, São Bernardo do Campo-SP, Brazil.
*** Escola Politécnica da Universidade de São Paulo, Departamento de Engenharia Metalúrgica e de Materiais, Av. Prof. Mello de Morais, 2463, CEP 05508-030, Cidade Universitária, Butantã, São Paulo-SP, Brazil.

ISSN 0011-9312 (print), 1938-159X (online)
11/000047/$5.00+$0.50/0

TABLE 1
Chemical Composition (wt%) of Super Duplex Stainless Steel UNS S32520

Cr	Ni	Mo	N	C	Mn	Cu	S	P	Si	Fe
24.90	6.500	4.040	0.218	0.024	0.867	1.399	0.001	0.046	0.295	Bal.

According to Tavares, et al.,[23] UNS S31803[(1)] DSS aging at 475°C for longer periods than 300 h, leads to changes in the fracture morphology from a completely ductile, with no cleavage facets in the ferrite phase, associated to solution-annealed samples, to a highly brittle one.

In this study, the mechanical and corrosion behavior of UNS S32520 SDSS samples, either solution-annealed or aged at 475°C for various periods that varied from 0.5 h to 1,032 h, were tested using microhardness, Charpy impact tests, electrochemical impedance spectroscopy (EIS), and cyclic polarization tests. Prior to aging at 475°C, all samples were solution-annealed at 1,200°C for 1 h. The goal of the study was to compare the sensibility of various types of tests, either mechanical or electrochemical, to the presence of alpha prime and to evaluate the effect of this phase on mechanical and corrosion properties.

EXPERIMENTAL PROCEDURES

Table 1 shows the chemical composition (wt%) of the UNS S32520 SDSS used in the present study. Initially, all the samples were solution-annealed at 1,200°C for 1 h, under nitrogen atmosphere, to have a homogeneous microstructure prior to aging treatment. Nitrogen atmosphere was used during aging treatments to avoid excessive oxidation and to prevent nitrogen loss from the SDSS. The aging treatments were performed at 475°C for various periods that varied from 0.5 h to 1,032 h, to obtain different alpha prime volumetric fractions in the material. After the aging treatment, the samples were quenched in water.

All tested samples had their surfaces ground with silicon carbide (SiC) paper from no. 220 to no. 2,000. Samples used for microstructural characterization, electrochemical, and micro-hardness tests had their tested surfaces polished using diamond abrasive from 6 μm to 1 μm and then rinsed with ethyl alcohol (C_2H_5OH).

Microstructural characterization was carried out by immersing the samples for 15 s in a modified Behara solution, at (22 ± 1)°C, composed of 20 mL hydrochloric acid (HCl), 80 mL distilled water, and 1 g potassium metabisulfide ($K_2S_2O_5$). To this stock solution, 2 g of ammonium bifluoride (NH_4HF_2) were added just before the etching. Subsequently, the samples were rinsed with deionized water, ethyl alcohol, and dried under a hot air stream. The samples were observed using an optical microscope.

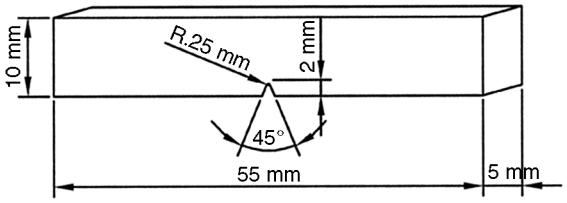

FIGURE 1. *Schematic V-notched sample for Charpy tests.*

Microhardness tests were carried out using a microdurometer with 0.5 kgf load, with 30 measurements being taken on each specimen. Reduced section Charpy impact tests were performed using a V-notched sample with dimensions of 55 by 10 by 5 mm, as Figure 1 illustrates.

Electrochemical tests were carried out using a three-electrode cell setup, with a platinum wire as counter electrode and a saturated calomel electrode (SCE) as reference electrode. The electrolyte used was 0.6 M sodium chloride (NaCl) at (22 ± 1)°C.

EIS measurements were carried out using a Gamry EIS 300[†] frequency response analyzer coupled to a potentiostat. The EIS measurements were performed at the open-circuit potential (OCP). The amplitude of the sinusoidal potential signal was 10 mV and the investigated frequency was from 100 kHz to 10 mHz, with an acquisition rate of 10 points per decade. The EIS measurements were obtained prior to the cyclic polarization tests. Cyclic potentiodynamic anodic polarization data were collected at a scan rate of 1 mV/s in the range from the OCP until the current density reached 1 mA/cm^2 when the scanning direction was reversed, and the tests were terminated when the potential reached the OCP initially measured. After polarization tests, some samples had their tested surface analyzed using scanning electron microscopy.

RESULTS AND DISCUSSION

Figure 2 shows micrographs of UNS S32520 SDSS samples, either solution-annealed or aged for 1,032 h. In the micrographs, alpha prime cannot be observed, because its small size and the similarity of the scattering amplitude of both chromium and iron diminish its detection even with techniques like x-ray diffraction and electron diffraction in the transmis-

[(1)] UNS numbers are listed in *Metals and Alloys in the Unified Numbering System*, published by the Society of Automotive Engineers (SAE International) and cosponsored by ASTM International.
[†] Trade name.

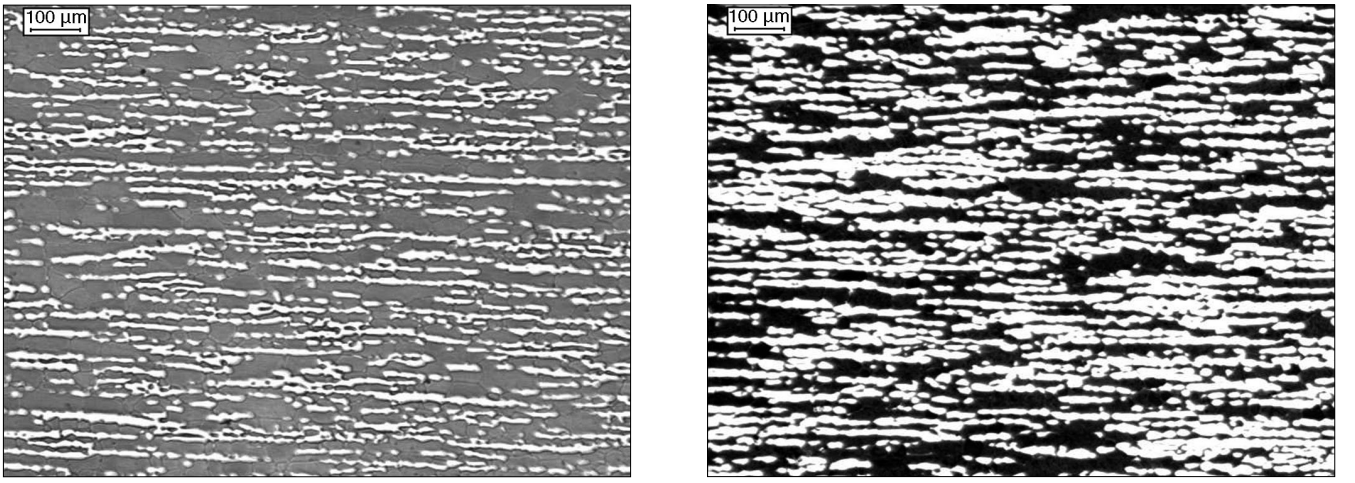

FIGURE 2. *Typical microstructure of UNS S32520 SDSS: (a) solution-annealed and (b) aged at 475°C for 1,032 h. Both micrographs show ferrite (dark gray) and austenite (white) phases.*

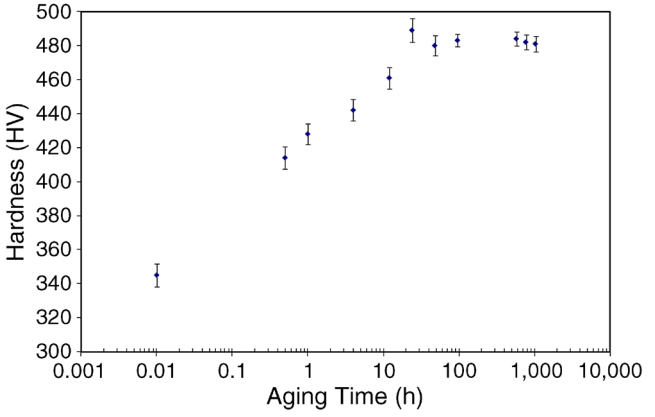

FIGURE 3. *Hardness profile for solution-annealed and aged samples at 475°C. The solution-annealed sample was represented by an aging time of 0.01 h. Results presented correspond to the mean of 30 measurements on each sample, and the vertical bars show the mean and standard deviation for each heat treatment condition.*

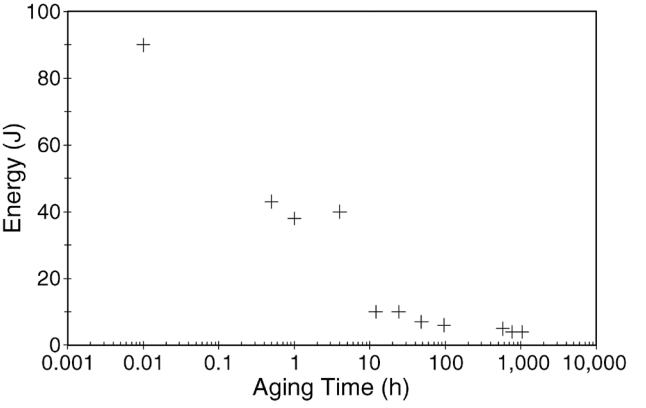

FIGURE 4. *Charpy impact test. Results for samples solution-annealed (0.01 h) and aged at 475°C samples.*

sion electron microscope.[24-25] Only two phases can be seen—the ferrite phase, which corresponds to the dark phase and the austenite phase, which corresponds to the white one. Both phases are aligned to the rolling direction in the observed surface.

The microhardness test results shown in Figure 3 indicate a gradual increase in hardness with aging time up to 24 h, when a maximum is reached, suggesting that alpha prime formation was completed. For longer aging periods, the hardness was fairly stable.

Absorbed energy values measured by the impact test for the 475°C aged samples during various times are shown in Figure 4. As it can be seen, a huge decrease in the absorbed energy was associated to samples aged for only 0.5 h, showing high susceptibility of this property to the alpha prime phase. Toughness degradation from the increasing amount of alpha prime with aging time is inferred from the results presented in this figure. As the amount of alpha prime increases, dislocation blockage also increases, leading to embrittlement.[26-27]

The solution-annealed fractured surface showed morphology typical of ductile fracture, with large and predominant dimples areas, as Figure 5(a) shows. The transition from a predominant ductile fracture to a brittle one is clearly seen in Figures 5(b) and (c), with decreased quantities of dimples. Clusters of alpha prime must have led to brittle fracture behavior. For aging periods longer than 12 h, the fractured surface showed a large amount of cleavage surfaces, typical of brittle fracture.

EIS results are shown in Figures 6(a) and (b) as Nyquist and Bode phase angle diagrams, respectively, for various aging times. High phase angles, typical of passive materials, are seen over a large frequency range. This is because of the much larger propor-

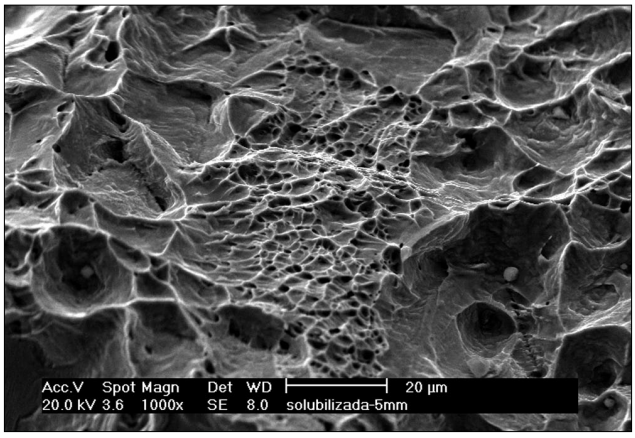

(a)

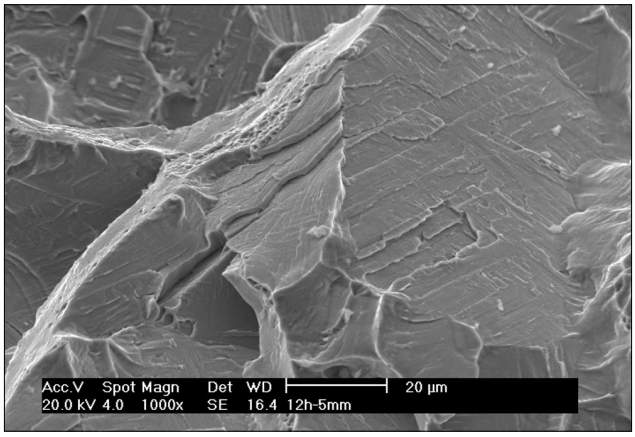

(b)

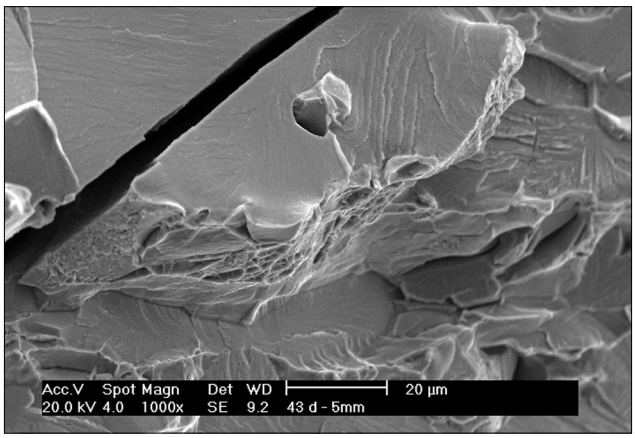

(c)

FIGURE 5. *Scanning electron microscopy micrographs of fractured areas of UNS S32520 SDSS: (a) solution-annealed sample, showing large amounts of dimples, typical of ductile fracture; (b) sample aged for 12 h showing brittle and ductile fracture; (c) sample aged for 1,032 h with large amount of cleavage surfaces, typical of brittle fracture.*

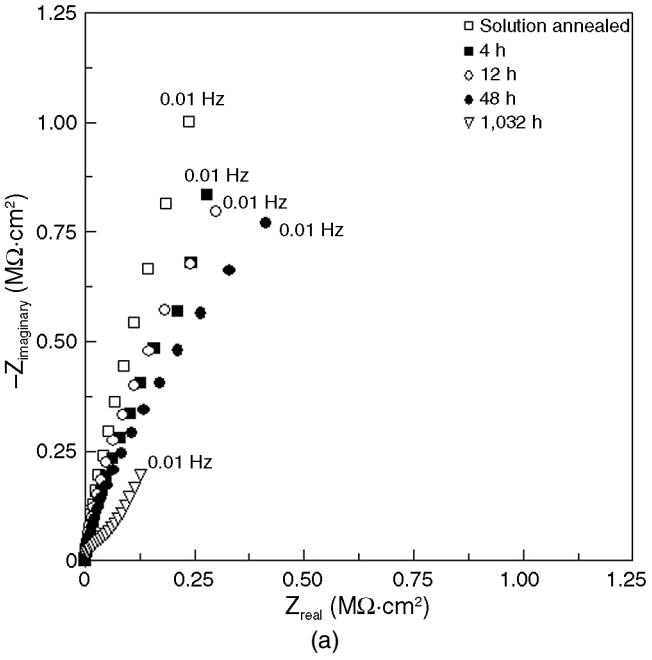

(a)

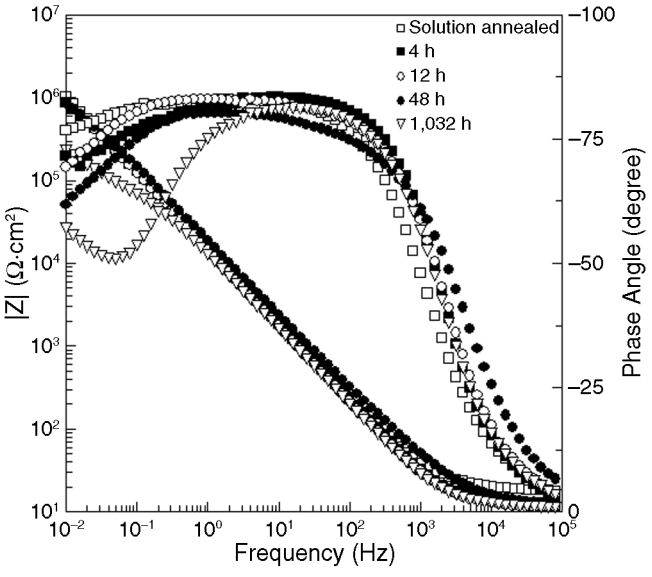

(b)

FIGURE 6. *(a) Nyquist and (b) Bode phase angle diagrams of samples of UNS S32520 solution-annealed and aged at 475°C for 1,032 h. Results obtained in 0.6 M NaCl solution.*

tion of the passive area at the surface, comparatively to the very low size of alpha prime. The impedance slightly decreased with aging time, and no significant changes could be detected for samples aged for shorter periods than 1,032 h. This result shows that the EIS is not a proper technique to detect the effects of alpha prime on the localized corrosion resistance of SDSS.

EIS results of samples aged for 1,032 h show a second time constant at low frequencies, which could be a result of corrosion processes at the exposed substrate at the defects in the passive film. However, the literature[27-28] has associated the two time constants usually found in stainless steels to the duplex structure of the passive layer, with an inner, chromium-rich layer and an outer, iron-rich layer.

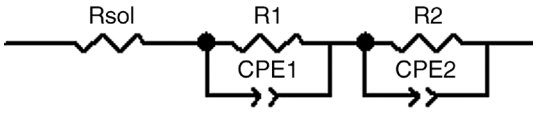

FIGURE 7. *Electrical equivalent circuits used to fit the Bode phase diagrams.*

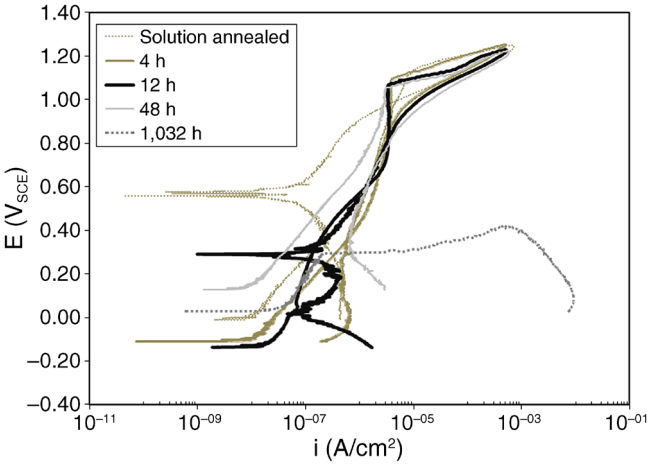

FIGURE 8. *Cyclic potentiodynamic polarization curves obtained for UNS S32520 in 0.6 M NaCl solution.*

EIS results were fitted using electrical equivalent circuits, and the best results were obtained with the equivalent circuit shown in Figure 7. It is proposed that the R1-CPE1 pair, corresponding to high-frequency data, is associated to the oxide and transfer processes and charging of the double layer at the oxide-electrolyte interface, whereas the R2-CPE2 pair corresponds to the low-frequency data and is related to charge-transfer processes at the stainless steel substrate-oxide interface and charging of the double layer. The results of fitting for the equivalent circuit components are shown in Table 2. In all cases, the agreement between experimental and fitted data was very good. The CPE exponents associated with the R1-CPE1 pair were between 0.8 and 0.9 for all tested samples. The CPE exponents related to the R2-CPE2 pair were around 1 for the solution-annealed samples and for the samples aged at 475°C for 4, 12 and 48 h. The samples aged for 1,032 h presented a lower value, around 0.9.

EIS results suggest that not only the resistance of the oxide layer and at the oxide-electrolyte interface, but also the charge-transfer process at the substrate-eletrolyte interface, decrease with aging time, suggesting a decreased corrosion resistance with the increase of alpha prime. The results also show that phase angles at low frequencies decreased with aging time. The results indicated that the passive layer becomes increasingly less protective because of rising amounts of defects caused by alpha prime precipitation during aging treatments.[26]

Cyclic potentiodynamic polarization curves are presented in Figure 8 and support the EIS results, also showing that the resistance to localized corrosion decreases with aging time. The film resistance to breakdown largely decreased from 12 h to 48 h showing that the material is progressively more prone to localized corrosion.

Very low current densities, which is typical of passive materials, and high pitting potentials (around 1.15 V_{SCE}) were obtained for the solution-annealed samples. These high pitting potentials found in this work can be associated with the reaction of oxygen evolution; once it takes place, current densities increase and bubbles of oxygen, from O_2(g) formation, favor passive layer breakdown.[30] The pitting potential decreased progressively with aging times up to 96 h at 475°C, as shown in Figure 9. For aging treatments higher than 96 h, the pitting potential diminishes drastically. The removal of chromium content from the ferrite matrix by alpha prime precipitation hinders the chromium redistribution in the matrix and, consequently, the repassivation process. Surface observation after polarization tests, Figure 10, shows that all aged samples are prone to localized attack, and the pits' density and depth increase with aging time as the amount of alpha prime phase also increases.

CONCLUSIONS

❖ The alpha prime phase might be detected indirectly by either mechanical or electrochemical methods, but the mechanical test, mainly the Charpy impact test, was the most susceptible to alpha prime presence

TABLE 2

Values of Resistance and Constant Phase Element Obtained for the Super Duplex Stainless Steel UNS S32550 Solutions Annealed and Solution-Annealed and Then Aged for 4, 12, 32, and 1.032 h at 475°C

	Rsol ($\Omega \cdot cm^2$)	CPE1 ($cm^{-2}s^{-n}\ \Omega$)	n1	R1 ($\Omega \cdot cm^2$)	CPE2 ($cm^{-2}s^{-n}\ \Omega$)	n2	R2 ($\Omega \cdot cm^2$)
Solution-annealed	18.69	3.75×10^{-5}	0.82	1.21×10^{5}	1.60×10^{-5}	0.99	6.18×10^{6}
Aged for 4h	12.79	2.54×10^{-5}	0.88	1.25×10^{5}	1.73×10^{-5}	0.98	4.15×10^{6}
Aged for 12h	11.37	2.70×10^{-5}	0.86	3.29×10^{5}	2.23×10^{-5}	0.99	4.15×10^{6}
Aged for 48 h	12.54	2.35×10^{-5}	0.81	2.13×10^{5}	1.75×10^{-5}	0.98	2.11×10^{6}
Aged for 1.032 h	11.59	1.96×10^{-5}	0.90	6.72×10^{4}	5.77×10^{-5}	0.92	9.72×10^{5}

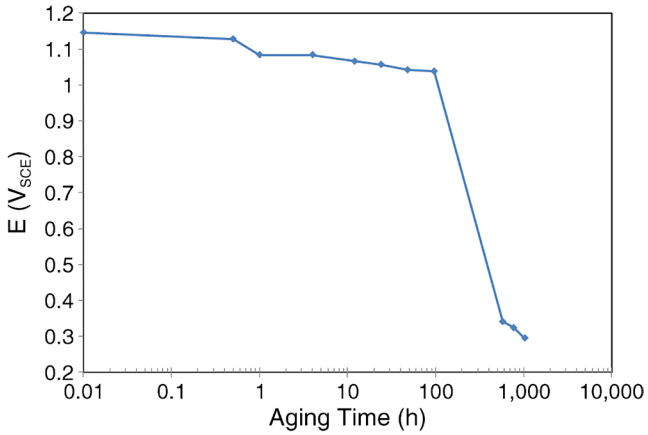

FIGURE 9. *Pitting potential for solution-annealed and aged at 475°C samples.*

among the tests used. Changes in pitting potential were only detected for samples with aging times longer than 96 h, and for the EIS, 1,032 h of aging was necessary to detect the alpha prime effect. However, the propensity to repassivation decreased in the samples aged for 48 h comparative to those aged for 12 h. Electrochemical tests also showed the deterioration of the oxide layer resistance, with decreased pitting potential, as a result of chromium impoverishment of ferritic matrix caused by alpha prime formation.

❖ The Charpy impact test was the most sensitive among the tests adopted in this study to detect alpha prime phase in the UNS S3250 SDSS. Samples aged only for 0.5 h showed a large reduction in fracture toughness. The hardness gradually increased with aging time until 24 h, indicating completion of alpha prime formation. Transition from a predominant ductile fracture, found in the solution-annealed sample, to a brittle fracture occurred with increasing aging times. It was also observed that the dimples, typical of ductile fracture, almost disappeared in the samples with longer aging times. It can be concluded that mechanical tests were more sensitive than the electrochemical methods adopted to determine the presence of alpha prime.

ACKNOWLEDGMENTS

The authors acknowledge CNEN for the financial support to T.F. Fontes and Fundação de Amparo à Pesquisa (FAPESP) for the financial support to M. Terada (Grant 08/54836-4). M. Magnani is acknowledged for scanning electron microscopy micrographs of pitting corrosion. Architect M.A. Roggero is also acknowledged for Charpy scheme drawing.

REFERENCES

1. G.W. Fan, J. Liu, P.D. Han, G.J. Qiao, *Mater. Sci. Eng. A* 515 (2009): p. 108.
2. J.S. Cheon, I.S. Kim, *J. Nucl. Mater.* 278 (2000): p. 96.

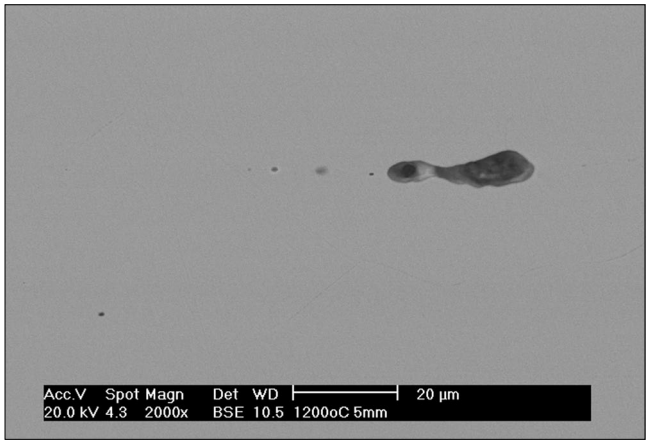

(a)

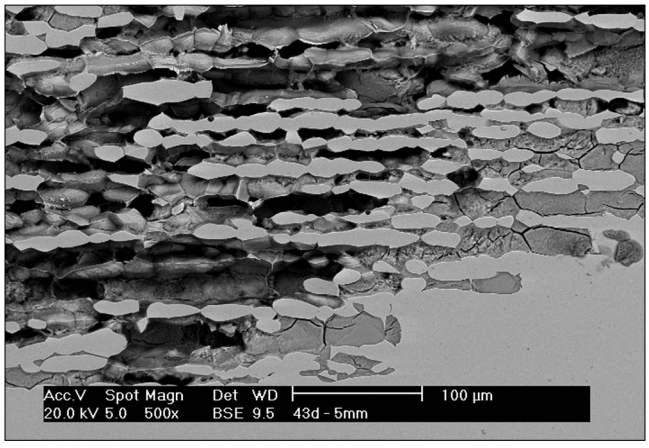

(b)

FIGURE 10. *Scanning electron microscopy micrographs of samples (a) solution-annealed and (b) aged for 1,032 h. Surfaces after polarization tests in 0.6 M NaCl solution.*

3. V. Di Cocco, E. Franzese, F. Iacoviello, S. Natali, *Eng. Fract. Mech.* 75 (2008): p. 705.
4. F. Iacoviello, F. Casari, S. Gialanella, *Corros. Sci.* 47 (2005): p. 909.
5. F. Iacoviello, M. Boniardi, G.M. La Vecchia, *Int. J. Fatigue* 21 (1999): p. 957.
6. C.-J. Park, H.-S. Kwon, *Mater. Chem. Phys.* 91 (2005): p. 355.
7. H.D. Solomon, L.M. Levinson, *Acta Metall.* 26 (1978): p. 429.
8. P.J. Grobner, *Metal. Trans.* 4A (1973): p. 251.
9. H.M. Chung, O.K. Chopra, "Microstructures of Cast-Duplex Stainless Steel after Long-Term Aging," Proc. 2nd Environmental Degradation of Materials in Nuclear Power Systems—Water Reactors (LaGrange Park, IL: American Nuclear Society, 1985), p. 289.
10. S. Cícero, J. Setién, I. Gorrochategui, *Nucl. Eng. Des.* 239 (2009): p. 16.
11. V. Calonne, C. Berdin, B. Saint-Germain, S. Jayet-Gendrot, *J. Nucl. Mater.* 327 (2004): p. 202.
12. R.M. Fisher, E.J. Dullis, K.G. Carroll, *Trans. Metall. Soc. AIME (J. Met.)* 197 (1953): p. 690.
13. R.O. Williams, H.W. Paxton, *J. Iron Steel Inst.* 185 (1957): p. 358.
14. A. Gironès, L. Llanes, M. Anglada, A. Mateo, *Mater. Sci. Eng. A* 367 (2004): p. 322.
15. M.B. Cortie, A.H. Pollak, *Mater. Sci. Eng. A* 199 (1995): p. 153.
16. J.K. Sahu, U. Krupp, R.N. Ghosh, H.-J. Christ, *Mater. Sci. Eng. A* 508 (2009): p. 1.
17. D. Chandra, L.H. Schwartz, *Metal. Trans.* 2 (1971): p. 511.
18. A. Isalgué, M. Anglada, *J. Mater. Sci.* 25 (1990): p. 4977.
19. M. Anglada, J. Rodriguez, A. Isalgué, *Scr. Metal.* 23 (1989): p. 1633.

20. M.M. Ura, A.F. Padilha, N. Alonso, "Influência da fase alfa linha (a') sobre a resistência à corrosão por pite em aços inoxidáveis dúplex" [Influence of Alpha Prime Phase on Pitting Corrosion Resistance of Duplex Stainless Steels], 1995 49th ABM Annual Congresss (São Paulo, Brazil: ABM, 1995), p. 337-349.
21. M. Terada, "Estudo da fragilização de 475 °C nos aços inoxidáveis ferríticos DIN W. Nr. 1.4575 (28%Cr-4%Ni-2%Mo-Nb) e Incoloy MA 956 (20%Cr-5%Al-Ti-Y_2O_3)" [Embrittlement at 475°C in Ferritic Stainless Steels DIN W. Nr. 1.4575 (28%Cr-4%Ni-2%Mo-Nb) and Incoloy MA 956 (20%Cr-5%Al-Ti-Y_2O_3)] (MSc thesis, University of São Paulo, Brazil, 2003).
22. T.F. Fontes, "Efeito da fase alfa linha nas propriedades mecânicas e de resistência à corrosão do aço inoxidável duplex UR N52+" [Alpha Prime Effect on Mechnical Properties and Corrosion Resistance of UR 52N+ Duplex Stainless Steel] (MSc thesis, University of São Paulo, Brazil, 2009).
23. S.S.M. Tavares, M.R. Da Silva, J.M. Neto, *J. Alloy. Compd.* 313 (2000): p. 168.
24. S. Kawaguchi, N. Sakamoto, G. Takano, F. Mtsuda, Y. Kikuchi, L. Mráz, *Nucl. Eng. Des.* 174 (1997): p. 273-285.
25. M. Martins, S.M. Rossitti, M. Ritoni, L.C. Casteletti, *Mater. Charact.* 58 (2007): p. 909-916.
26. M. Terada, A.F. Padilha, A.M.P. Simões, H.G. De Melo, I. Costa, *Mater. Corros.* 60 (2009): p. 852.
27. N.E. Hakiki, S. Boudin, B. Rindot, M. Da Cunha Belo, *Corros. Sci.* 37 (1995): p. 1809.
28. N.E. Hakiki, M. Da Cunha Belo, *J. Electrochem. Soc.* 145 (1998): p. 3821.
29. J.E.G. González, J.C. Mirza-Rosca, *J. Electronal. Chem.* 471 (1999): p. 109.
30. R. Magnabosco, N. Alonso-Falleiros, *Corrosion* 61, 2 (2005): p. 130, doi:10.5006/1.3278167.